The EMBO Journal (2008) 27, 361–372 | © 2008 European Molecular Biology Organization | Some Rights Reserved 0261-4189/08
www.embojournal.org

THE EMBO JOURNAL

EMBO open

Rapid and bi-directional regulation of AMPA receptor phosphorylation and trafficking by JNK

Gareth M Thomas, Da-Ting Lin, Mutsuo Nuriya[1] and Richard L Huganir*

Department of Neuroscience, Howard Hughes Medical Institute, Johns Hopkins University School of Medicine, Baltimore, MD, USA

Jun N-terminal kinases (JNKs) are implicated in various neuropathological conditions. However, physiological roles for JNKs in neurons remain largely unknown, despite the high expression level of JNKs in brain. Here, using bioinformatic and biochemical approaches, we identify the AMPA receptor GluR2L and GluR4 subunits as novel physiological JNK substrates *in vitro*, in heterologous cells and in neurons. Consistent with this finding, GluR2L and GluR4 associate with specific JNK signaling components in the brain. Moreover, the modulation of the novel JNK sites in GluR2L and GluR4 is dynamic and bi-directional, such that phosphorylation and de-phosphorylation are triggered within minutes following decreases and increases in neuronal activity, respectively. Using live-imaging techniques to address the functional consequence of these activity-dependent changes we demonstrate that the novel JNK site in GluR2L controls reinsertion of internalized GluR2L back to the cell surface following NMDA treatment, without affecting basal GluR2L trafficking. Taken together, our results demonstrate that JNK directly regulates AMPA-R trafficking following changes in neuronal activity in a rapid and bi-directional manner.

The EMBO Journal (2008) **27,** 361–372. doi:10.1038/sj.emboj.7601969; Published online 10 January 2008
Subject Categories: neuroscience; signal transduction
Keywords: LTD; LTP; MAPK; synaptic transmission

Introduction

Mitogen-activated protein kinases (MAPKs) mediate cellular responses to diverse signals, including growth factors, pro-inflammatory cytokines and high osmolarity (Pearson *et al*, 2001). However, MAPKs are also highly expressed in brain, where they regulate various forms of synaptic plasticity. For example, the extracellular-signal regulated kinases (ERKs) play key roles in several forms of Long-term potentiation (LTP), while p38 MAPK may mediate certain forms of Long-term depression (LTD) (Zhu *et al*, 2002; Thomas and Huganir, 2004).

Another major MAPK subgroup is the cJun N-terminal kinases (JNKs), named for their ability to phosphorylate the transcription factor cJun. The JNK family comprises three related gene products: JNK1 and JNK2 are widely expressed, while JNK3 is restricted to brain, plus a limited set of non-neuronal tissues (Barr and Bogoyevitch, 2001; Pearson *et al*, 2001). Much work on JNKs in neurons has focused on their roles in neuropathology. In particular, mice lacking JNK3 show diminished excitotoxic cell death (Yang *et al*, 1997) and reduced effects of cerebral ischemia-hypoxia (Kuan *et al*, 2003), while JNK inhibitors show therapeutic promise by reducing cell death in many neuropathological models (Xia *et al*, 2001; Waetzig and Herdegen, 2005). Despite this focus on their neuropathological roles, the high neuronal expression of JNKs suggests that these kinases play important physiological roles. This hypothesis is strengthened by reports that JNKs, particularly the JNK1 isoform, exhibit high constitutive activity in brain (Lee *et al*, 1999; Coffey *et al*, 2002; Kuan *et al*, 2003; Bjorkblom *et al*, 2005; Brecht *et al*, 2005). Furthermore, neuronal JNK-dependent effects in both physiological and pathological conditions correlate poorly with cJun phosphorylation, suggesting key roles for additional JNK substrates (Bjorkblom *et al*, 2005; Besirli *et al*, 2005). Recently, JNKs have been reported to regulate synaptic plasticity (Chen *et al*, 2005; Zhu *et al*, 2005). However, direct JNK substrates that might control synaptic transmission remain to be identified. The lack of definitive physiological neuronal JNK substrates has also hindered investigation into how JNKs, and the phosphatases that oppose them, regulate downstream targets in response to changes in neuronal activity.

AMPA-type glutamate receptors (AMPA-Rs) mediate the majority of fast excitatory neurotransmission in the brain. Regulation of AMPA-Rs plays critical roles in forms of synaptic plasticity such as long-term potentiation (LTP) and long-term depression (LTD) (Malinow and Malenka, 2002; Song and Huganir, 2002). Native AMPA-Rs are multimers, formed from combinations of four different subunits, named Glutamate Receptors (GluRs) 1–4. GluRs are grouped, according to length and homology of their intracellular C-terminal tails, into 'long' and 'short' classes. Alternative splicing of the GluR2 and GluR4 mRNAs generates both long and short-tailed versions of these AMPA-Rs while GluR1 and GluR3 have only a long-tailed and a short-tailed version, respectively. Phosphorylation sites and interaction motifs present only in specific AMPA-R subunits allow regulation of specific receptor subpopulations, which then play key roles in specific forms of plasticity. For example, AMPA-Rs containing the GluR1 and GluR2 (short form) subunits are reported to play

*Corresponding author. Department of Neuroscience, Howard Hughes Medical Institute, Johns Hopkins University School of Medicine, 725 N Wolfe Street, Hunterian 1001, Baltimore, MD 21205, USA.
Tel.: +1 410 955 4050; Fax: +1 410 955 0877;
E-mail: rhuganir@jhmi.edu
[1]Present address: Department of Pharmacology, School of Medicine, Keio University, 35 Shinanomachi, Shinjuku, Tokyo 160-8582, Japan

Received: 5 November 2007; accepted: 3 December 2007; published online: 10 January 2008

specific roles in hippocampal LTP and LTD, respectively (Malinow and Malenka, 2002; Song and Huganir, 2002).

Using bioinformatics techniques we identified consensus sites for JNK family MAPKs on the intracellular regions of two long-tailed AMPA-R subunits; GluR4 and the long-tailed splice form of GluR2, GluR2L. Specific mechanisms that regulate GluR2L and GluR4 are largely unknown, despite the fact that these receptors contribute significantly to AMPA-R transmission during development (Zhu *et al*, 2000; Esteban *et al*, 2003; Kolleker *et al*, 2003). We therefore investigated the possibility that GluR2L and GluR4 might be novel neuronal JNK substrates, and that JNK-dependent phosphorylation might specifically regulate these AMPA-Rs.

Here we show that GluR2L and GluR4 are indeed JNK substrates *in vitro*, in heterologous cells and in neurons. We demonstrate that in neurons, basal JNK activity maintains high constitutive phosphorylation of both GluR2L and GluR4, but several stimuli that increase glutamatergic signaling trigger rapid dephosphorylation of these receptors at JNK sites. Conversely, blocking neuronal activity with TTX rapidly increases JNK-mediated phosphorylation of both GluR2L and GluR4. This suggests that JNKs, and the phosphatases that oppose them, form a bi-directional system to rapidly respond to neuronal activity changes. Using live-imaging methods to investigate the functional consequence of GluR2L phosphorylation by JNKs we report that the novel JNK phosphorylation site on GluR2L plays a key role in controlling activity-dependent GluR2L trafficking. These findings identify novel physiological JNK substrates in mature neurons, revealing a previously unappreciated role for these kinases in regulation of specific AMPA-Rs.

Results

One of the few known neuronal JNK substrates, the microtubule-associated protein MAP2, is phosphorylated by JNK1 at unspecified sites (Chang *et al*, 2003; Bjorkblom *et al*, 2005). A large-scale proteomic study revealed vast numbers of *in vivo* phosphorylated sites in synaptic preparations (Trinidad *et al*, 2006) and we inspected this report for MAP2 *in vivo* phosphorylation sites. As expected, we found phosphorylated MAP2 sites homologous to phosphorylated sites on the well-characterized JNK substrate, cJun. This suggested that further JNK substrates might contain sequences homologous to these cJun/MAP2 sites (Figure 1A). We therefore probed the Scansite database (http://scansite.mit.edu) with a consensus motif derived from the conserved MAP2/cJun phospho-motif (Figure 1A). Strikingly, the 'hits' included several proteins with key roles

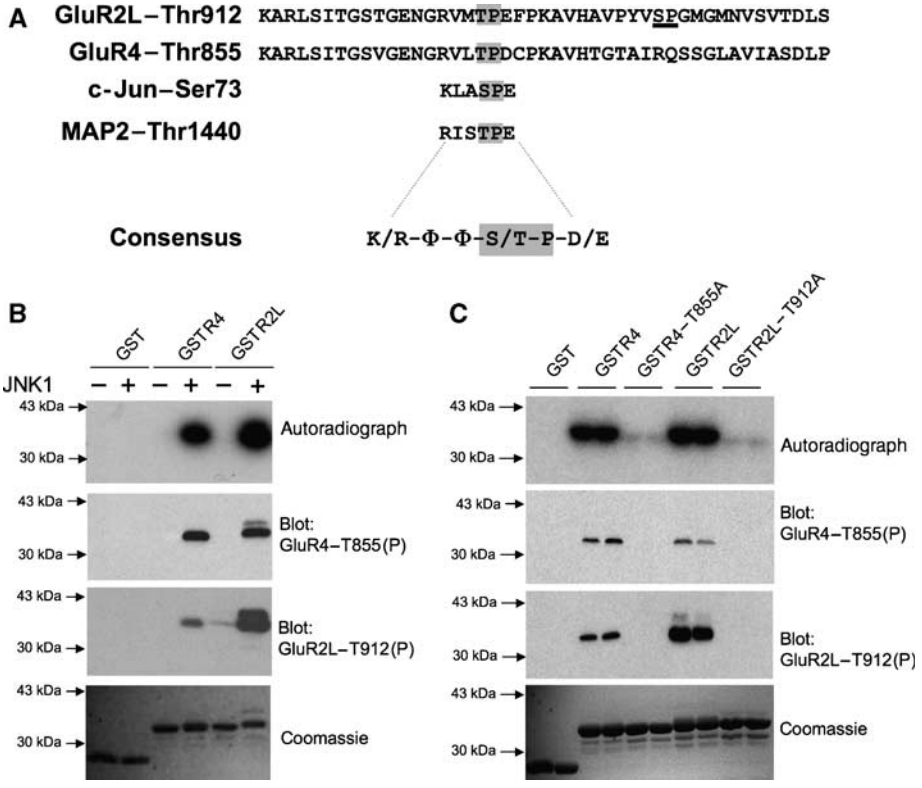

Figure 1 JNK1 phosphorylates a novel site on AMPA-R C-terminal tails *in vitro*. (**A**) GluR2L and GluR4 sequences, from the GluR4 phosphorylation site Ser842 to the C-terminus, are aligned to indicate conserved potential MAPK phosphorylation sites (GluR2L-Thr912, GluR4-Thr855, shown in gray). These sequences show clear homology to sites on the JNK substrates cJun and MAP2 that are phosphorylated *in vivo*. A consensus (basic residue at $N-3$, aliphatic/polar/uncharged residues (Φ) at $N-2$ and $N-1$, proline at $N+1$, acidic residue at $N+2$, where N is the phosphorylated residue) is shown. A second potential MAPK site (Ser926) in GluR2L is underlined. (**B**) JNK1 phosphorylates GluR2L and GluR4 C-termini *in vitro*. Autoradiograph (top), immunoblots with GluR2LThr912(P) antibody (second panel) or GluR4Thr855(P) antibody (third panel) and Coomassie Blue staining (bottom) of purified GST, GST-GluR4 or GST-GluR2L used in kinase assays in the presence (+) or absence (−) of active JNK1. (**C**) JNK1 phosphorylates GST-GluR4 and GST-GluR2L at Thr-855 and Thr-912, respectively. GST, GST-GluR4, GST-GluR2L and point mutants (Thr-Ala) of these GluRs at the potential JNK phosphorylation site were incubated with active JNK1 and $[\gamma]^{32}$P-ATP. Autoradiograph (top), GluR2LThr912(P) immunoblot (second panel), GluR4Thr855(P) immunoblot (third panel) and Coomassie Blue staining (bottom) of duplicate determinations per condition.

in synaptic regulation (see Discussion). In particular, the cJun/MAP2 motif perfectly matched regions within the C-terminal tails of two AMPA-Rs, GluR4 and the long splice form of GluR2 (GluR2L). The GluR4 (Thr855) and GluR2L (Thr912) JNK consensus motifs are conserved across species (data not shown).

We therefore examined whether GST-fusions of GluR4 and GluR2L tails could serve as JNK substrates in *in vitro* kinase assays. Indeed, JNK1 phosphorylated both GST-GluR2L and GST-GluR4 extremely effectively *in vitro* (Figure 1B), with Km values approaching those of the known JNK substrate ATF2 (data not shown). Mutation of GluR2L-Thr912 or GluR4-Thr855 to alanine abolished JNK1 phosphorylation of these tails (Figure 1C), indicating that Thr855 and Thr912 were the sites phosphorylated by JNK1. In contrast, other MAPK family enzymes with known roles in synaptic regulation (ERK2, p38alpha and the MAPK-related cyclin family kinase CDK5) barely phosphorylated these GluR tails *in vitro*, though each kinase efficiently phosphorylated its known substrates (data not shown).

Two phospho-antibodies were developed to monitor GluR2L-Thr912 and GluR4-Thr855 phosphorylation. Both antibodies were highly phospho-specific, recognizing their GluR antigens only after phosphorylation with JNK1 *in vitro* (Figure 1B). Neither antibody recognized the GluR2L or GluR4 alanine mutants (Figure 1C). The GluR4-Thr855(P) antibody also recognized GluR2L-Thr912(P) and the GluR2L-Thr912(P) antibody weakly recognized GluR4-Thr855(P) (Figure 1C). This was not unexpected since these sites are highly similar (Figure 1A).

To examine whether JNKs could regulate GluR2L phosphorylation in mammalian cells we transfected HEK293T cells with GluR2L cDNA and added 0.5 M sorbitol, an osmotic shock that activates JNK (Bagowski *et al*, 2003). Blotting of lysates with GluR2L-Thr912(P) antibodies revealed immunoreactivity only in GluR2L-transfected cells (Figure 2A). Immunoreactivity was weak in unstimulated cells but was increased dramatically by sorbitol treatment (Figure 2A). A JNK inhibitor, SP600125 (Bennett *et al*, 2001), prevented the sorbitol-induced increase in phosphoThr912 signal. Inhibitors of other MAPK pathways (SB203580, which inhibits p38/SAPK2, and U0126, which prevents ERK activation) or Roscovitine, a cyclin-dependent kinase (cdk) inhibitor did not affect sorbitol-induced GluR2L-Thr912 phosphorylation (Figure 2A). This suggests that endogenous HEK293T cell JNKs phosphorylate GluR2L-Thr912.

Using similar methods we examined GluR4 phosphorylation in transfected HEK293T cells. Due to cellular bands recognized by the GluR4-Thr855(P) antibody we immunoprecipitated GluR4 (Supplementary Figures S1, S2) to examine its phosphorylation in isolation. PhosphoThr855 immunoreactivity (Figure 2B) was only detected in immunoprecipitates from GluR4-transfected cells. PhosphoThr855 immunoreactivity was weak in unstimulated cells, was increased dramatically by sorbitol treatment, and was greatly reduced by SP600125 but not by ERK pathway, p38 or cdk inhibitors. These data suggest that endogenous HEK293T cell JNKs phosphorylate GluR4 at Thr855.

As a complementary method to modulate JNK signaling we used the JNK-binding domain (JBD) of the scaffold protein JIP1 (JNK-interacting protein-1, also known as Islet-brain-1; Dickens *et al*, 1997; Whitmarsh *et al*, 1998; Xia *et al*, 2001). JIP proteins scaffold multiple JNK pathway kinases and increase efficacy of signaling via this pathway. JBD over-expression draws JNK away from its upstream activators and prevents phosphorylation of downstream JNK substrates (Dickens *et al*, 1997; Xia *et al*, 2001). Consistent with this model, myc-JBD co-transfection greatly reduced sorbitol-induced GluR2L-Thr912 phosphorylation. In contrast, sorbitol-induced GluR2L-Thr912 phosphorylation was dramatically higher in cells co-transfected with myc-JNK1 (Figure 2C). Sorbitol-induced GluR4-Thr855 phosphorylation was also reduced by myc-JBD, and augmented by myc-JNK1 (Figure 2D), supporting the hypothesis that JNKs phosphorylate GluR2L and GluR4 in heterologous cells.

To examine endogenous GluR2L and GluR4 phosphorylation we immunoprecipitated these AMPA-Rs from cultured cortical neurons and from rat brain membrane fractions using specific antibodies (Supplementary Figures S1, S2). GluR2L and GluR4 immunoprecipitates showed strong immunoreactivity with GluR2L-Thr912(P) and GluR4-Thr855(P) antibodies, respectively, and lambda phosphatase treatment confirmed that both signals were phospho-specific (Supplementary Figure S2). GluR2L is not detected in GluR4 co-immunoprecipitates (or vice versa) from either cultured neurons or rat brain membrane fractions (Supplementary Figure S1). Thus, GluR2L and GluR4 are phosphorylated, at Thr912 and Thr855 respectively, in cultured neurons and in rat brain.

JNK activity, particularly attributed to JNK1, is constitutively high in brain (Lee *et al*, 1999; Coffey *et al*, 2002). Consistent with this, basal phosphorylation of GluR2L-Thr912 and GluR4-Thr855 was high in unstimulated neurons. However, basal GluR2L-Thr912 and GluR4-Thr855 phosphorylation were both lowered substantially by SP600125, but not by other MAPK pathway inhibitors, or by a cdk5 inhibitor (Figure 3A). A structural analog of SP600125 that poorly inhibits JNK affected neither GluR2L-Thr912 nor GluR4-Thr855 phosphorylation (Supplementary Figure S3). These results suggest that high basal JNK activity (Lee *et al*, 1999; Coffey *et al*, 2002; Kuan *et al*, 2003; Bjorkblom *et al*, 2005; Brecht *et al*, 2005) mediates the majority of basal GluR2L-Thr912 and GluR4-Thr855 phosphorylation in neurons. Interestingly, membrane and synaptosomal fractions from juvenile rat brain showed markedly higher phosphoJNK signals, though JNK levels were similar across fractions (Supplementary Figure S4). This suggests that active JNKs are enriched in membrane fractions, where they are ideally situated to maintain high basal phosphorylation of AMPA-Rs and other synaptic substrates.

As in heterologous cells, we used a JBD-based approach to modulate JNK signaling and examined GluR2L/GluR4 phosphorylation. A cell-permeant peptide consisting of the HIV-1 TAT sequence fused to a JBD fragment (TAT-JBD) also dramatically reduced both GluR2L-Thr912 and GluR4-Thr855 phosphorylation (Figure 3B). In contrast, a TAT-JBD peptide with mutations in two residues critical for JNK binding did not affect phosphorylation of either GluR2L-Thr912 or GluR4-Thr855 (Supplementary Figure S3).

The reduction of GluR2L/GluR4 phosphorylation by JIP1-based intervention provided further evidence that JNK phosphorylates these AMPA-Rs in neurons and implicated JIP-dependent JNK pathway scaffolds in regulation of these AMPA-Rs. Indeed, we detected JNK1, JIP1 and the upstream

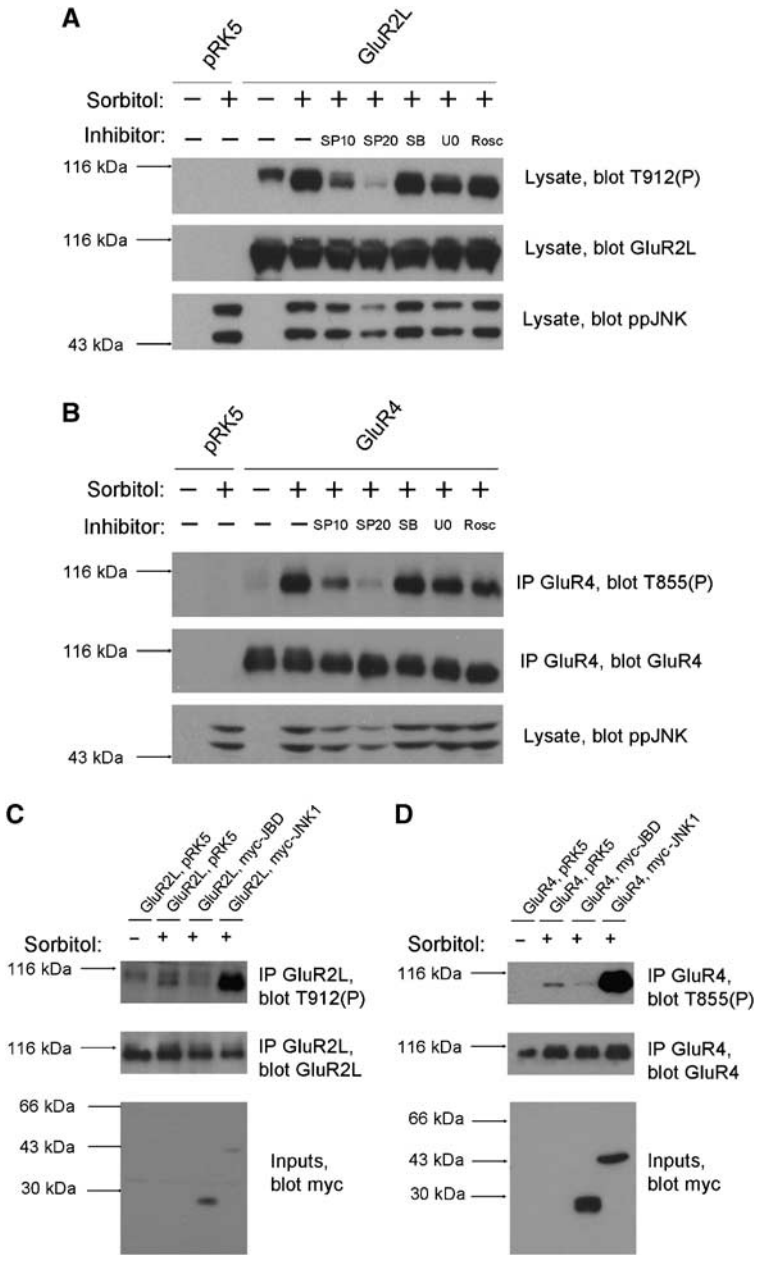

Figure 2 Endogenous JNK phosphorylates GluR4-Thr855 and GluR2L-Thr912 in transfected cells. (**A**) HEK 293T cells transfected with vector (pRK5) or GluR2L cDNA were pre-incubated with DMSO vehicle (−) or the indicated inhibitors (SP10: 10 μM SP600125; SP20: 20 μM SP600125; SB: 10 μM SB 203580; U0: 10 μM U0126; Rosc: 10 μM Roscovitine) prior to stimulation with (+) or without (−) 0.5 M Sorbitol. Lysates were blotted for phosphoThr912 (top), total GluR2L (middle) and active, phosphorylated JNK (phosphoJNK, bottom). SP600125 blocks the kinase activity of JNK but not its phosphorylation by upstream kinases. Thus SP600125 minimally affects phosphoJNK signals but the catalytic activity of JNK itself is still inhibited. (**B**) As (A), except that cells were transfected with empty vector or GluR4 cDNA and GluR4 immunoprecipitates were blotted for phosphoThr855 (top) and total GluR4 (second panel). Lysates were blotted for phosphoJNK (bottom). (**C**) HEK293T cells were co-transfected with GluR2L cDNA plus either pRK5 vector, myc-tagged JNK-binding domain (myc-JBD) or myc-tagged JNK1 (myc-JNK1) prior to stimulation with (+) or without (−) 0.5 M Sorbitol for 30 min. GluR2L immunoprecipitates were blotted for phosphoThr912 (top), total GluR2L (middle) and lysates were blotted to detect myc-tagged proteins (bottom). (**D**) As (C), except that cells were transfected with empty vector or GluR4 cDNA plus pRK5 vector or myc-tagged JNK-binding domain (myc-JBD) or JNK1 (myc-JNK1) and GluR4 immunoprecipitates were blotted for phosphoThr855 (top), total GluR4 (middle) and lysates were blotted for myc-tagged proteins (bottom).

JNK activator MAP kinase kinase-7 (MKK7) in GluR2L and GluR4 immunoprecipitates from rat brain membranes (Figure 3C and D). Other JNK isoforms (JNK2 and JNK3) were not detected (data not shown). This suggests that JNK pathway kinases, scaffolded by JIP1, associate with AMPA-Rs in neurons and thus provides a molecular explanation for how JNK might phosphorylate GluR2L/GluR4. The specific presence of JNK1 in such complexes is consistent with reports that JNK1 accounts for much of the basal JNK activity in brain (Coffey *et al*, 2002; Bjorkblom *et al*, 2005; Brecht *et al*, 2005).

This isoform-specific enrichment of JNK1 in AMPA-R complexes led us to examine the subcellular distribution of JNK pathway components and AMPA-Rs (Supplementary Figure S5). Synaptosomal and Post-synaptic density (PSD) fractions showed clear presence of JNK1, JNK3, MKK7 and JIP1. In contrast, JNK2 was largely excluded from PSD

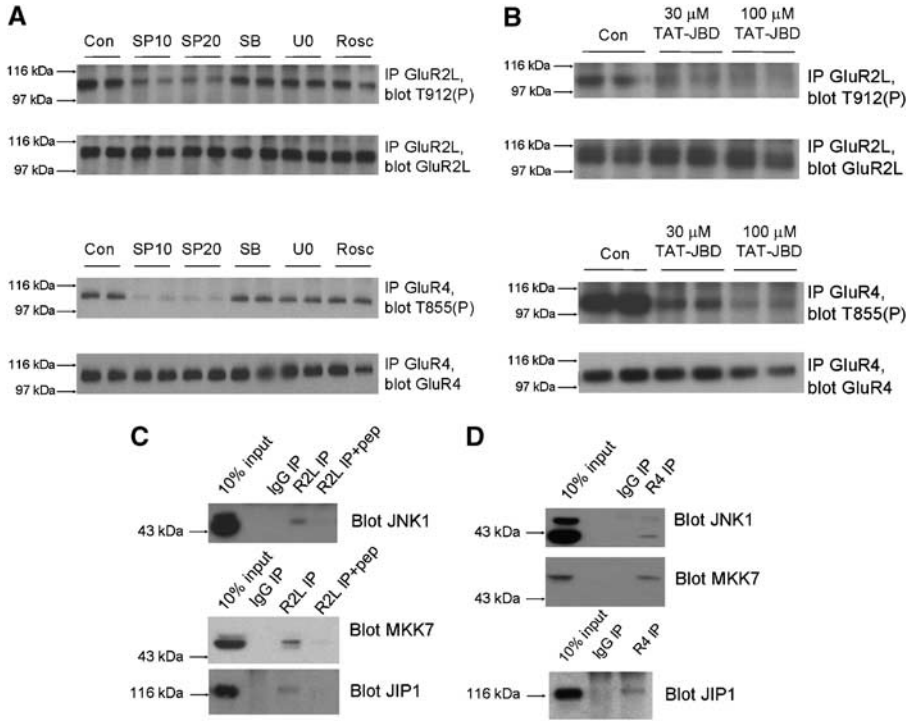

Figure 3 JNK-JIP1 complexes mediate high basal phosphorylation of GluR2L-Thr912 and GluR4-Thr855 in neurons. (**A**) Cortical neurons (DIV 15–20) were washed into aCSF containing DMSO vehicle control ('Con') or the indicated inhibitors (SP10: 10 μM SP600125; SP20: 20 μM SP600125; SB: 10 μM SB 203580; U0: 10 μM U0126; Rosc: 10 μM Roscovitine) prior to lysis. GluR2L immunoprecipitates were blotted for phosphoThr912 (Top) and GluR2L (second panel). GluR2L-Thr912 phosphorylation relative to total GluR2L signal (normalized to control, 100%): SP10: 53.5±5.4%, $N=6$; SP20: 35.4±5.4%, $N=6$; SB: 95.7±18.2%, $N=5$; U0: 89.8±18.2%, $N=6$; Rosc: 86±24.5%, $N=5$). GluR4 immunoprecipitates were blotted for phosphoThr855 (third panel) or GluR4 (bottom). GluR4-Thr855 phosphorylation relative to total GluR4 (normalized to control, 100%). SP10: 19.8±3.9%; SP20: 24.2±2.9%; SB: 93.7±9.1%; U0:86.9±4.8%; Rosc: 102.7±12.1% ($N=4$ for all treatments). (**B**) as *A* except that neurons were incubated for 1 h with the indicated concentrations of TAT-JBD peptide. (**C**) GluR2L immunoprecipitates (pre-incubated with or without antigenic peptide) were prepared from membrane fractions from juvenile (P17–20) rats and blotted for JNK pathway components. (**D**) As (C) except that GluR4 immunoprecipitates were prepared.

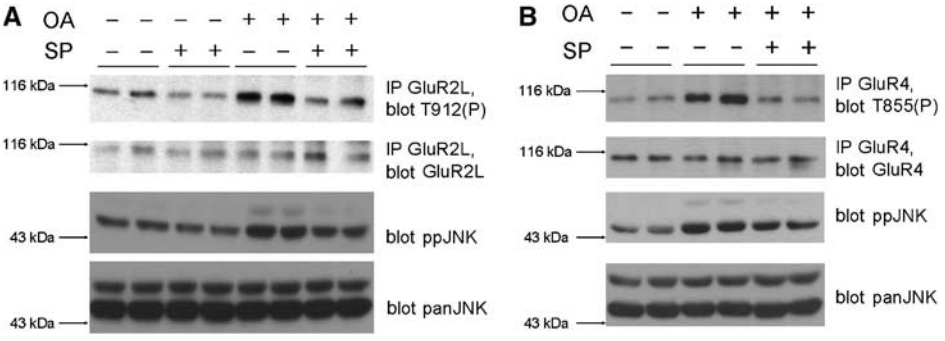

Figure 4 JNK dynamically regulates GluR2L-Thr912 and GluR4-Thr855 phosphorylation in neurons. (**A**) Cortical neurons were incubated in aCSF in the presence (+) or absence (−) of 10 μM SP600125 for 1 h and then stimulated for 10 min with 1 μM okadaic acid (+) or left unstimulated (−). GluR2L immunoprecipitates were blotted for phosphoThr912 (top), GluR2L (second panel), phosphoJNK (third panel) or panJNK (bottom). GluR2L-Thr912 phosphorylation relative to total GluR2L (normalized to control, 100%) SP: 53.5±5.4%, $N=6$; OA: 197.8±32.8%, $N=4$; OA+SP: 64.0±32.2%, $N=4$. (**B**) as *A* except that GluR4 immunoprecipitates were prepared and blotted for phosphoThr855 (top) or GluR4 antibody (second panel). GluR4-Thr855 phosphorylation relative to total GluR4 (normalized to control, 100%) OA: 209.2±49.1%, $N=6$; OA+SP: 90.9±26.6%, $N=5$.

fractions, consistent with data suggesting that JNK2 functions pre-synaptically (Chen *et al*, 2005).

Phosphorylation is a rapid and reversible process and so we investigated whether GluR2L-Thr912 or GluR4-Thr855 phosphorylation are dynamically regulated in neurons. Treatment of neurons with the phosphatase inhibitor okadaic acid increased levels of phosphoJNK, GluR2L-Thr912(P) (Figure 4A) and GluR4-Thr855(P) (Figure 4B). Okadaic acid-induced increases in both GluR2L-Thr912(P) and GluR4-Thr855(P) were JNK inhibitor-sensitive.

Pathological stimuli alter neuronal JNK substrate phosphorylation (Yang *et al*, 1997; Fogarty *et al*, 2003), but it is less clear how more subtle changes, particularly in glutamatergic signaling, might regulate neuronal JNK substrates. We therefore examined whether glutamatergic signaling regulates GluR2L/GluR4 phosphorylation. Bath application

of NMDA, which specifically activates NMDA-type glutamate receptors, caused rapid and dramatic dephosphorylation of both GluR2L-Thr912 and GluR4-Thr855 (Figure 5A). Both sites were also dephosphorylated following brief treatment with bicuculline (which blocks inhibitory transmission, thus increasing synaptic glutamate release; Figure 5B), withdrawal of the NMDA-R antagonist APV or treatment with AMPA (Supplementary Figure S6).

The treatments that decreased GluR2L-Thr912 and GluR4-Thr855 phosphorylation act in distinct ways, but share the ability to increase glutamatergic signaling. We therefore wondered whether reagents that act in an opposite manner (i.e. to inhibit glutamatergic signaling) might differentially affect GluR2L/GluR4 phosphorylation. Indeed, inhibiting neuronal activity with TTX clearly increased phosphorylation of JNK, GluR2L-Thr912 and GluR4-Thr855 (Figure 5B). This suggests that phosphorylation of synaptic JNK targets is regulated by a novel mechanism and that the JNK pathway, and the phosphatases that oppose it, function as a rapid detector of changes in neuronal activity.

The rapid dephosphorylation of GluR2L-Thr912 and GluR4-Thr855 triggered by NMDA or bicuculline (Figure 5A and B) occurred without changes in phosphoJNK (Figure 5B and C) suggesting that dephosphorylation is due not to decreased JNK activity but to increased protein phosphatase activity. Indeed, addition of okadaic acid immediately prior to NMDA treatment prevented NMDA-induced GluR2L-Thr912 and GluR4-Thr855 dephosphorylation (Figure 5A). NMDA-induced dephosphorylation was not prevented by low okadaic acid concentrations that selectively inhibit PP2A-type phosphatases (Supplementary Figure S6), suggesting that dephosphorylation of GluR2L-Thr912 and GluR4-Thr855 is regulated by a PP1 family phosphatase.

NMDA treatment also triggers dephosphorylation of GluR1, another long-tailed AMPA-R subunit, at Ser845, and this dephosphorylation accompanies GluR1 internalization

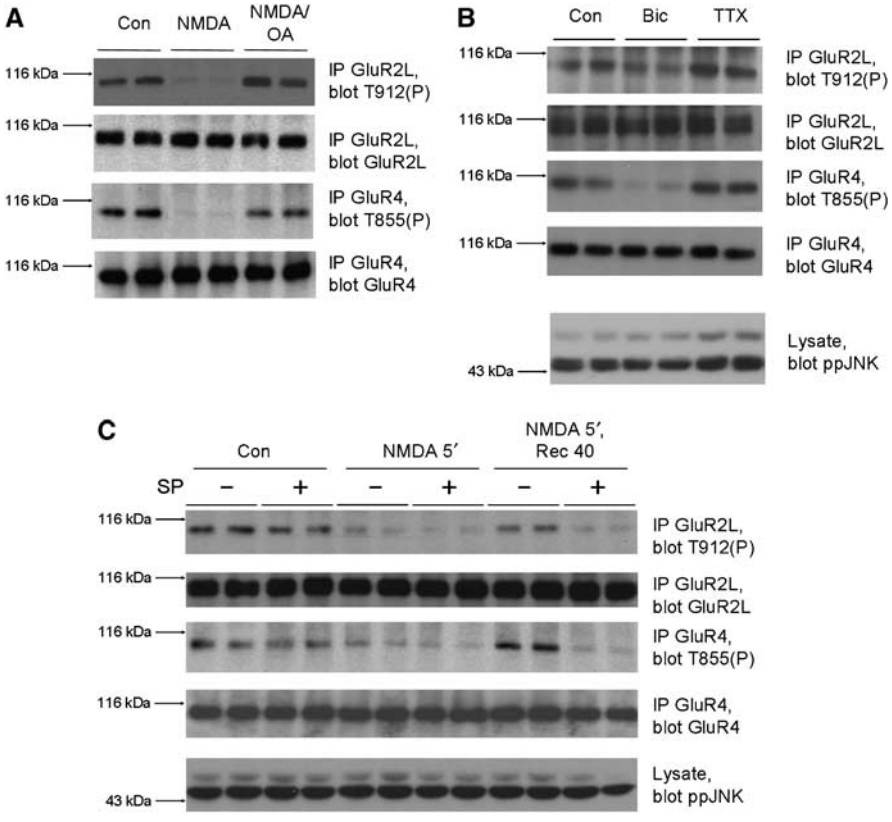

Figure 5 Neuronal activity changes rapidly and bi-directionally modulate GluR2L-Thr912 and GluR4-Thr855 phosphorylation in neurons. (**A**) Cortical neurons were incubated in aCSF for 1 h, treated for 10 min with 1 μM okadaic acid or DMSO vehicle, and then stimulated for 10 min with 30 μM NMDA, or were left unstimulated (Con). GluR2L immunoprecipitates were blotted for phosphoThr912 (top) or GluR2L (lower panel). GluR2L-Thr912 phosphorylation relative to total GluR2L (normalized to control, 100%) NMDA: 36.8±9.0%, $N=6$; NMDA+OA: 92.1±12%, $N=6$. GluR4 immunoprecipitates were blotted for phosphoThr855 (third panel) or GluR4 (bottom). GluR4-Thr855 phosphorylation relative to total GluR4 (normalized to untreated control, 100%) NMDA: 28.5±6.3%, $N=6$; NMDA+OA: 89.3±17.4%, $N=6$. (**B**) Cortical neurons were stimulated with 20 μM Bicuculline (Bic) or 1 μM Tetrodotoxin (TTX) for 20 min. Immunoprecipitates were prepared and blotted as in (A). Lysates were blotted to detect phosphoJNK. GluR2L-Thr912 phosphorylation relative to total GluR2L (normalized to control, 100%) Bic: 61.9±12.8%, $N=4$; TTX: 142.2±16.9%, $N=4$. GluR4-Thr855 phosphorylation relative to total GluR4 (normalized to control, 100%) Bic: 42.5±21.5%, $N=4$; TTX: 176.1±40.4%, $N=4$. (**C**) Cortical neurons were washed into aCSF in the presence (+) or absence (−) of 10 μM SP600125 for 1 h prior to stimulation for 5 min with 20 μM NMDA. Cells were lysed or washed into aCSF in the absence of NMDA for a further 40 min prior to lysis. Control cells were left unstimulated. GluR2L immunoprecipitates were blotted for phosphoThr912 (top), or GluR2L (second panel). GluR2L-Thr912 phosphorylation relative to total GluR2L (normalized to control, 100%) Con/SP: 75.2±3.3%, $N=4$; NMDA: 58.4±7.0%, $N=4$; NMDA/SP: 30.1±1.8%, $N=4$; Rec: 85.0±12.2%, $N=4$; Rec/SP: 27.5± 6.6%, $N=4$. GluR4 immunoprecipitates were blotted for phosphoThr855 (third panel), or GluR4 (bottom). GluR4-Thr855 phosphorylation relative to total GluR4 (normalized to control, 100%) Con/SP: 65.6±22.0%, $N=4$; NMDA: 49.3±10.8%, $N=4$; NMDA/SP: 30.2±9.7%, $N=4$; Rec: 87.4±10.7%, $N=4$; Rec/SP: 38.3±9.9%, $N=4$. Lysates were blotted for phosphoJNK (bottom). Note that the effect of SP600125 on GluR2L-Thr912 and GluR4-Thr855 phosphorylation is more marked after NMDA washout than under basal conditions (compare lanes 1,2 with 3,4 and 9,10 with 11,12).

(Lee *et al*, 1998; Ehlers, 2000). Subsequent washout of NMDA allows GluR1-Ser845 re-phosphorylation and GluR1 returns to the plasma membrane (Ehlers, 2000). We therefore examined whether NMDA treatment and washout might induce a similar dephosphorylation/re-phosphorylation cycle for GluR2L-Thr-912 and/or GluR4-Thr855. As previously, NMDA treatment led to dephosphorylation of both GluR2L-Thr-912 and GluR4-Thr855. Both sites were rephosphorylated, essentially to basal levels, following NMDA washout (Figure 5C). Importantly, rephosphorylation of GluR2L-Thr912 and GluR4-Thr855 was highly sensitive to JNK inhibition (Figure 5C). This suggests that JNKs are critical for rapid rephosphorylation of GluR2L-Thr912 and GluR4-Thr855 following NMDA washout.

Changes in GluR1 phosphorylation following NMDA treatment and washout accompany alterations in GluR1 trafficking (Ehlers, 2000). The strikingly similar dephosphorylation/re-phosphorylation of GluR2L-Thr912 (and GluR4-Thr855) (Figure 5C) led us to examine the role of Thr912 phosphorylation in GluR2L trafficking. We therefore modified GluR2L with a pH-sensitive GFP (super-ecliptic pHluorin) at its N-terminus. The pHluorin tag fluoresces at neutral pH (e.g. when present on the cell surface and exposed to extracellular medium), but at acidic pH (as encountered when the receptor internalizes to acidic endosomes) fluorescence is quenched (Ashby *et al*, 2004; Lin and Huganir, 2007). pH-GluR2L expressed efficiently in neurons and was efficiently targeted to the cell surface (Supplementary Figure S7). Expression levels of pH-GluR2Lwt, pH-GluR2L-T912A (a non-phosphorylatable mutant) and pH-GluR2L-T912D (a putative phospho-mimetic mutant) were similar in neurons (data not shown). In addition, pH-GluR2Lwt, pH-GluR2L-T912A and pH-GluR2L-T912D surface expression levels were similar, as judged by immunostaining (Supplementary Figures S7, S8) or by biotinylation methods to isolate cell surface fractions (data not shown). Furthermore, pH-GluR2Lwt, pH-GluR2L-T912A and pH-GluR2L-T912D were similarly targeted to excitatory synapses (Supplementary Figure S7). These results suggested that the status of GluR2L-Thr912 affects neither expression of this AMPA-R, nor its targeting to the cell surface or to synapses. Moreover, SP600125 addition during live-imaging experiments caused no run-up or rundown of fluorescence for either pH-GluR2Lwt, pH-GluR2L-T912A or pH-GluR2L-T912D, suggesting that although JNK inhibition triggers GluR2L-Thr912 dephosphorylation (Figure 3A), modulation of Thr912 phosphorylation does not affect basal GluR2L trafficking. This hypothesis was supported by Fluorescence Recovery After Photobleach (FRAP) experiments (Supplementary Figure S9).

Following brief NMDA treatment the robust basal fluorescence of pH-GluR2L decreased dramatically in both the cell soma and in dendrites (Figure 6A, Supplementary Figure S10), consistent with receptor internalization from the cell surface to acidic endosomes as reported for pH-GluR2 (Ashby *et al*, 2004; Lin and Huganir, 2007). NMDA-induced decreases in dendritic pHGluR2L fluorescence occurred with similar kinetics to those in the cell soma (Supplementary Figure S10). As reported elsewhere (Ashby *et al*, 2004; Lin and Huganir, 2007), NMDA perfusion predominantly internalizes diffuse, extra-synaptic AMPA-Rs (Supplementary Figure S10). Following NMDA washout, pH-GluR2L fluorescence recovered, reaching levels observed prior to NMDA perfusion (Figure 6A and C). Fluorescence recovery was largely due to recycling of endocytosed pH-GluR2L back to the plasma membrane as recovery was largely ($>75\%$) prevented by photobleach of surface pH-GluR2L prior to NMDA treatment (data not shown).

Interestingly, pH-GluR2Lwt, pH-GluR2L-T912A and pH-GluR2L-T912D internalized at similar rates and to similar degrees following NMDA perfusion, suggesting that the status of GluR2L-Thr912 did not influence receptor endocytosis (Supplementary Figure S11). Moreover, NMDA-induced pH-GluR2Lwt internalization was unaltered by SP600125 (Figure 6C). However, SP600125 dramatically attenuated re-insertion of pH-GluR2Lwt to the plasma membrane, with $<40\%$ of initial fluorescence recovered, even 60 min after NMDA washout in both the cell soma and in dendrites (Figure 6B, C and G, Supplementary Figure S10).

This suggested that JNK signaling is critical for pH-GluR2L recycling to the plasma membrane. This might be due to direct modulation of pH-GluR2L-Thr912 by JNK, or because SP600125 prevents JNK from phosphorylating a trafficking protein that controls pH-GluR2L recycling. Strikingly, however, SP600125 did not prevent either pH-GluR2L-T912D (Figure 6D) or pH-GluR2L-T912A (Figure 6E) recycling, suggesting that the status of Thr912 was indeed critical for recycling. The specificity of SP600125 was further confirmed by examining recycling of pH-GluR2 (short form), which differs from pH-GluR2L only in its intracellular C-terminus. pH-GluR2 fluorescence reduced dramatically in response to NMDA (consistent with internalization) and recovered, essentially to initial levels, following NMDA washout in the presence of SP600125 (Figure 6F). Thus SP600125 prevents recycling of pH-GluR2Lwt, but not recycling of pH-GluR2L-T912A, pH-GluR2L-T912D or pH-GluR2 (Figure 6G).

Discussion

Despite the high neuronal expression of JNKs, physiological JNK targets in brain and their modes of regulation by neuronal activity have remained obscure. Here, using a bioinformatics-based approach, we identified two AMPA-R subunits as novel JNK substrates in developed neurons. We further showed that both AMPA-R subunits are regulated in a novel JNK-dependent manner in response to neuronal activity changes, and revealed a previously unappreciated role for JNK signaling in the control of AMPA-R trafficking. A schematic summarizing these results is shown in Figure 7.

Our initial interest in the novel GluR2L/GluR4 sites was aroused by their homology to phosphorylated sites in the JNK substrates cJun and MAP2 (Figure 1A, consensus sequence K/R-Φ-Φ-S/T-P-D/E, where Φ is an aliphatic/non-polar residue). Our findings that GluR2L and GluR4 are also phosphorylated by JNK at such sites suggest that K/R-Φ-Φ-S/T-P-D/E is a novel JNK consensus motif. We note that other synaptic proteins with key roles in AMPA-R regulation (e.g. SAP97, 4.1N, liprin-alpha3; Malinow and Malenka, 2002; Song and Huganir, 2002; Wyszinski *et al*, 2002) also contain K/R-Φ- Φ-S/T-P-D/E motifs. The possibility that such proteins may also be *in vivo* JNK substrates is intriguing.

To this point, roles for JNK in synaptic transmission have gone largely unreported. However, the GTPase Rap2 reportedly signals via JNK to regulate synaptic depotentiation (Zhu *et al*, 2005). Zhu *et al* reported that one AMPA-R subtype

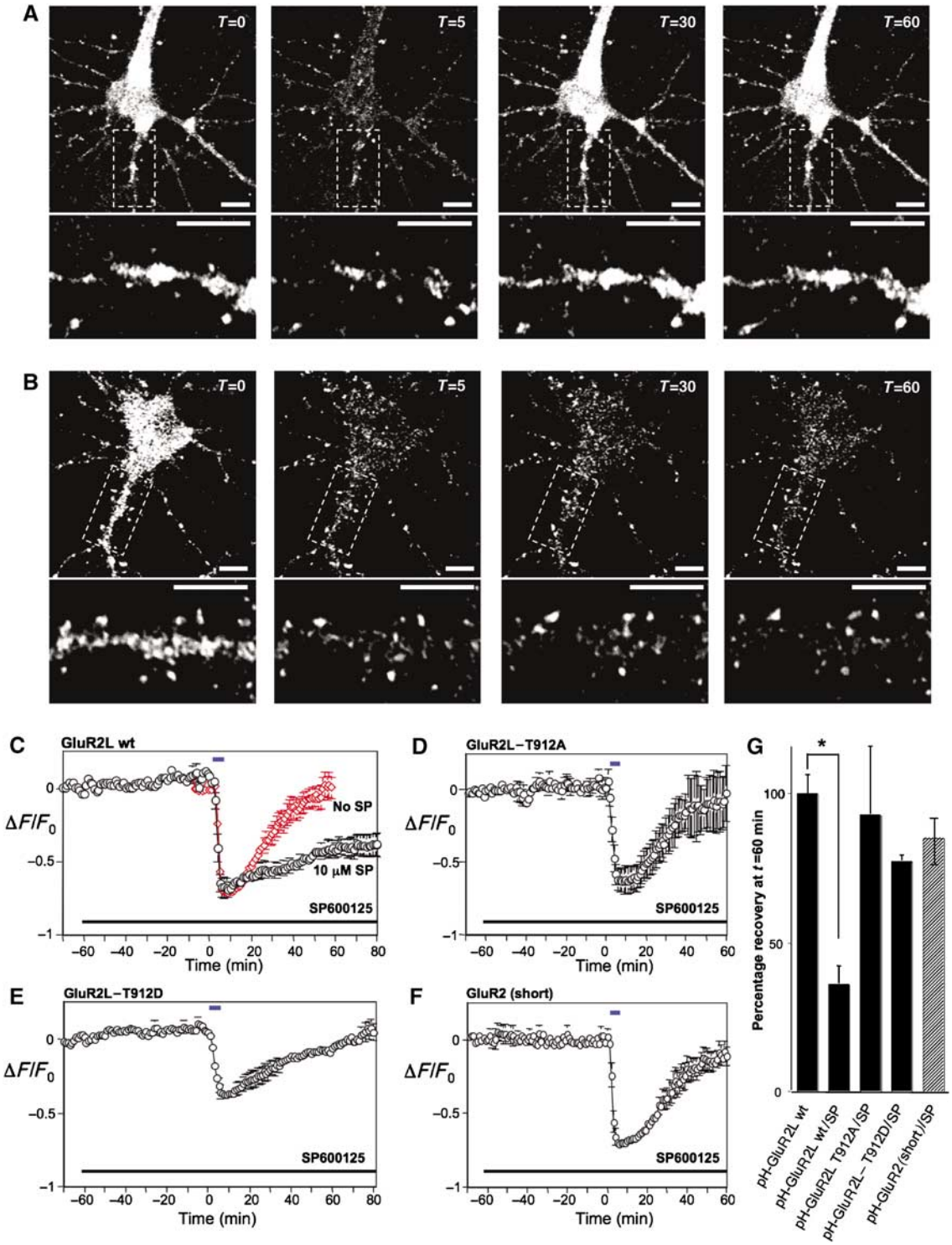

Figure 6 Live imaging of pHluorin-tagged GluR2L (pH-GluR2L) internalization and recycling. (**A**) Representative images of fluorescence change of a hippocampal neuron expressing pH-GluR2L, exposed at $t=0$ to 20 μM NMDA for 5 min and then allowed to recover following NMDA washout. Lower panels show enlargements of the dendritic region boxed in the upper panels. Scale bars = 10 μm. As reported elsewhere (Ashby *et al*, 2004), NMDA perfusion predominantly internalizes diffuse, extra-synaptic AMPA-Rs. The signal:noise ratio of dendritic fluorescence change is thus less robust, due to the contribution of clustered/punctate pHGluR2L that does not internalize following NMDA treatment. (**B**) As *A*, but for a neuron incubated for 1 h in the presence of 10 μM SP600125 prior to NMDA treatment. SP600125 was present during NMDA treatment and recovery. (**C**) Fluorescence change (mean ± s.e.m.) during initial incubation, perfusion with 20 μM NMDA for 5 min at $t=0$ min (blue bar) and washout, plotted for neurons in the presence of DMSO vehicle (red diamonds) or 10 μM SP600125 (black circles). SP600125 was present as indicated (black bar). (**D**) As *C*, but for neurons expressing pH-GluR2L-T912A. (**E**) As *C* but for neurons expressing pH-GluR2L-T912D. (**F**) As *C*, but for neurons expressing pH-GluR2(short). Data in *A–E* are plotted as mean ± s.e.m. for the following number of individual cells, from at least two platings of neurons: GluR2L wt: $N=8$; GluR2L wt + SP: $N=5$; GluR2L T912A: $N=3$; GluR2L T912D: $N=5$; GluR2 (short): $N=4$ (**G**) Fluorescence recovery, quantitated 1 h after NMDA washout in *B–E* (*$P<0.01$, Student *t*-test).

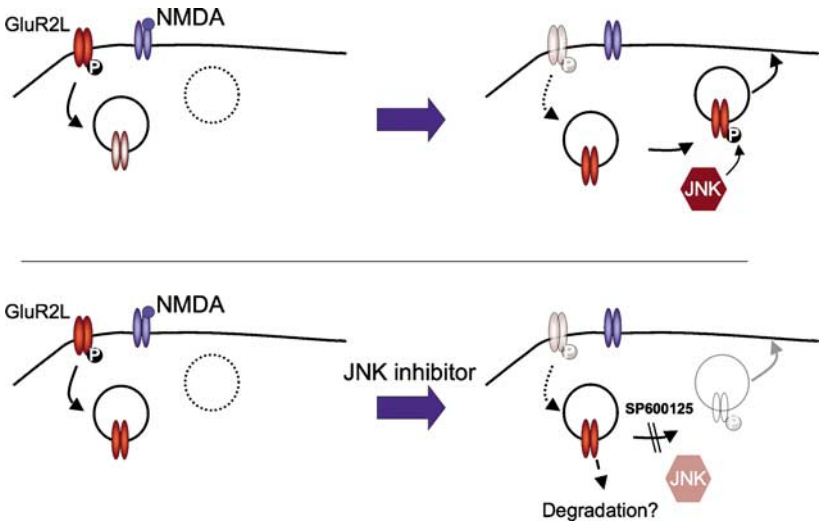

Figure 7 Phosphorylation of GluR2L by JNK controls activity-dependent reinsertion but is not required for basal recycling. NMDA-R activation triggers GluR2L internalization and Thr912 dephosphorylation. Following NMDA washout, high basal JNK activity catalyzes GluR2L-Thr912 rephosphorylation, allowing GluR2L re-insertion into the plasma membrane. JNK inhibition prevents rephosphorylation and the receptor cannot recycle. Basal (non-NMDA-dependent) recycling is unaffected by JNK inhibition.

removed from synapses by this putative Rap2-JNK pathway was GluR2L. We report here that JNK controls GluR2L re-insertion, but note several possible explanations for differences between our findings and those of Zhu *et al*.

Firstly, the two studies used different experimental systems, in which JNK may play different roles. However, Zhu *et al* relied heavily on overexpression of constitutively active signaling proteins, AMPA-Rs or both, which may not reflect the endogenous situation. In particular, Zhu *et al* reported that NMDA treatment activates Rap2 and overexpression of constitutively active Rap2 increases phosphoJNK. However, they presented no data that NMDA treatment activates JNK (Zhu *et al*, 2005), and we observe no JNK activation following NMDA treatment. Indeed, JNK activation by NMDA in cortical neurons is induced only by pathologically high NMDA concentrations that induce excitotoxicity (e.g. Borsello *et al*, 2003). This suggests that the NMDA-Rap2-JNK link proposed (but not demonstrated) by Zhu *et al* is unlikely to function physiologically, and that the small changes in phospho-JNK following Rap2 overexpression (Zhu *et al*, 2005) may be due to Rap2 effects on other pathways, which then indirectly affect JNK. Such indirect effects are well known when active small G proteins are overexpressed (e.g. McCarthy *et al*, 1995).

Rap2-induced changes in AMPA-R phosphorylation (Zhu *et al*, 2005) are also likely to be indirect and not mediated by JNK. Although Rap2 overexpression affects 'GluR2L-Ser842' phosphorylation (GluR2L-Ser899 following standard notation; a site homologous to GluR4-Ser842) (Zhu *et al*, 2005), this site is not a likely direct JNK substrate. Firstly, GluR2L-Ser899 does not lie in a consensus sequence for JNK or for any JNK pathway kinase. Moreover, while the use of crude lysates by Zhu *et al* means that their Ser899 phosphoantibody might also detect the homologous GluR4-Ser842 site, we find that JNK inhibition affects neither GluR4-Ser842 nor GluR2L-Ser899 phosphorylation in neurons (data not shown). Rap2-induced GluR2L-Ser899 (and perhaps GluR4-Ser842) phosphorylation (Zhu *et al*, 2005) is thus best accounted for by a kinase(s) distinct from JNK.

In contrast, our work mainly tracks endogenous AMPA-R phosphorylation in neurons and is supported by *in vitro* and heterologous cell studies. Both novel AMPA-R sites that we identify lie in excellent JNK consensus motifs and JNK phosphorylates both sites efficiently. Point mutation of each site eliminates both GluR2L and GluR4 phosphorylation by JNK. Phosphorylation of both GluR2L-Thr912 and GluR4-Thr855 is JNK-dependent in neurons and is most likely mediated by JNK1. This is consistent with other reports that basal neuronal JNK activity is high and is due mainly to JNK1 (Bjorkblom *et al*, 2005; Brecht *et al*, 2005). While a different JNK population (a different isoform or scaffold complex) may regulate the Rap2 pathway proposed (Zhu *et al*, 2005), some findings by Zhu *et al* may be due to indirect effects.

The rapid and bi-directional modulation of GluR2L-Thr912 and GluR4-Thr855 phosphorylation following neuronal activity changes is very interesting. Increases in neuronal activity promote dephosphorylation of both sites, while decreases in activity promote phosphorylation. This bi-directional modulation is similar to that recently reported for PSD-95 phosphorylation at Ser-295, which was also ascribed to JNK1 (Kim *et al*, 2007) and thus supports our model of neuronal JNK substrate phosphorylation, rather than that described by Zhu *et al*. Importantly, bi-directional modulation of neuronal JNK substrates may reflect a common mechanism allowing rapid feedback control of phosphorylation and function of multiple proteins involved in neurotransmission. Feedback mechanisms employed by neurons have drawn intense attention, most notably in the field of homeostatic plasticity (O'Brien *et al*, 1998; Turrigiano *et al*, 1998; Thiagarajan *et al*, 2005; Shepherd *et al*, 2006). However, forms of homeostatic plasticity described thus far all occur over long time courses (hours to days). Our report of a rapid response system controlled by JNKs (and phosphatases that oppose them) reveals a new mechanism used by neurons to respond bi-directionally to activity changes on the timescale of only a few minutes. Regulatory feedback of this type has parallels to adaptation in sensory systems, where distinct mechanisms

control rapid, short-term and long-term changes for multiple sensory modalities. Identification of further physiological neuronal JNK substrates may provide key insights into mechanisms used by neurons to rapidly adjust to different levels of activity.

Although GluR1-Ser845 dephosphorylation is implicated in GluR1 internalization (Ehlers, 2000; Lee *et al*, 2003), Thr912 dephosphorylation is unnecessary for GluR2L internalization. However, the status of GluR2L-Thr912 plays a key role in controlling GluR2L recycling to the plasma membrane following NMDA washout. Our finding that the non-phosphorylatable GluR2L-T912A mutant and the putative phospho-mimetic GluR2L-T912D mutant both override the SP600125-dependent block of GluR2L recycling is initially surprising. A possible explanation is that NMDA treatment triggers retention of internalized, dephosphorylated GluR2L by a protein that specifically binds 'Thr912-dephosphorylated' GluR2L. If this retention protein cannot bind the GluR2L-T912A and GluR2L-T912D mutants then these receptors would return to the cell surface. This explanation is not without precedent: for example, both S842A and S842D mutants of GluR4 traffic to synapses in the presence of high magnesium concentrations that prevent synaptic delivery of wildtype GluR4 (Esteban *et al*, 2003). An interaction that retains 'Ser842-dephosphorylated' GluR4 was postulated to explain these findings. Indeed, proteins that bind only dephosphorylated forms of other AMPA-Rs are already known; the multi-PDZ domain protein GRIP1 binds the GluR2 C-terminus only when GluR2 is dephosphorylated at Ser880 ('dephosphoSVKI'; Matsuda *et al*, 1999; Chung *et al*, 2000). Ser880 phosphorylation or mutations to non-phosphorylatable (AVKI) or phospho-mimetic (EVKI) residues ablate GRIP binding (Dong *et al*, 1997; Chung *et al*, 2000). It is therefore very possible that a GluR2L-dephosphoThr912 interactor might not recognize GluR2L-T912A or GluR2L-T912D. The identification of phospho-dependent AMPA-R interactors is an exciting area for future study, since such proteins likely play key roles in AMPA-R trafficking.

Our identification of two novel AMPA-R phosphorylation sites and the pathways that regulate their phosphorylation and dephosphorylation, plus the characterization of a novel functional role for this phosphorylation cycle increases our knowledge of the specificity of AMPA-R regulation and reveals new roles for neuronal JNK signaling. Since aberrant JNK signaling likely underlies several neuropathologies, the identification of physiological neuronal JNK targets will greatly increase our understanding of cellular processes that may become disregulated during pathological JNK hyperactivation. With this knowledge the likelihood of improved treatments for JNK-dependent neuropathological conditions is greatly increased.

Materials and methods

Materials and Methods are described only briefly here. Full details are available in Supplementary data.

cDNA clones

Full-length rat GluR4 and GluR2L, subcloned into the pRK5 mammalian expression vector, were used as PCR templates to generate GluR4 and GluR2L C-terminal tails, which were subcloned into the mammalian expression vector pCIS-GST. Point mutants of these constructs and full length GluR2L were generated by Quickchange (Stratagene, La Jolla, CA). The unique *BspEI* site in the rat GluR2 sequence was used to replace all except the C-terminus of GluR2L with a rat GluR2 'short' construct N-terminally tagged with pH-sensitive GFP (pHluorin; Ashby *et al*, 2004). Mouse JNK1beta1 was subcloned into pRK5 in frame with an N-terminal myc epitope. The JIP1 JNK-binding domain (JBD: Dickens *et al*, 1997) was PCR-amplified from a rat EST (Genbank Accession CK475933) and subcloned into myc-pRK5.

Purification of GST-GluR tails

GST-GluR tails were expressed in HEK 293T cells and affinity-purified.

In vitro JNK assay

Kinase reactions contained 2 μM GST or GST-GluR tails plus 5 ng of His-JNK1 or blank buffer. Incorporation of ^{32}P-radioactivity from [γ]^{32}P-ATP was detected by autoradiography.

GluR phosphorylation in HEK293T cells

HEK293T cells were transfected with full-length GluR2L or GluR4 cDNA. In some experiments, cells were co-transfected with GluR cDNA plus empty vector, myc-JBD or myc-JNK1 cDNAs. After 24 h recovery, cells were stimulated with 0.5 M Sorbitol for 30 min or left unstimulated. Kinase inhibitors were added to medium for 1 h prior to stimulation and remained during stimulation. Cells were lysed and GluR2L or GluR4 were immunoprecipitated. Immunoprecipitates were denatured in SDS sample buffer, subjected to SDS-PAGE, transferred to PVDF membrane and immunoblotted to examine AMPA-R phosphorylation. Bands were visualized by ECL.

GluR phosphorylation in cortical neurons

Cortical neurons were prepared from E18 rats. At 15–20 DIV, medium was replaced with artificial cerebrospinal fluid (aCSF) containing, in mM: 10 HEPES pH 7.4, 150 NaCl, 3 KCl, 2 $CaCl_2$, 1 Mg, 10 glucose and cells placed at 37°C for 1 h. In some experiments kinase inhibitors were added to aCSF during this period. For NMDA stimulations, neurons were washed into aCSF plus 1 μM TTX for 1 h and then treated with NMDA for 10 min. For okadaic acid treatments, this compound or DMSO vehicle was added to aCSF 10 min prior to NMDA stimulation. For NMDA treatment and recovery experiments, cells were washed into aCSF for 1 h as above and then stimulated for 5 min with 20 μM NMDA. aCSF was removed, cells were washed twice with aCSF plus 1 μM TTX and then allowed to recover at 37°C for 40 min. Following stimulations, cells were lysed and immunoprecipitates prepared as for HEK293T cells. For TTX and bicuculline treatments, cells remained in full medium and 1 μM TTX or 20 μM bicuculline (final concentrations) were added for 20 min prior to cell lysis.

Sucellular fractionation

Adult rat PSD fractions were prepared as described (Cho *et al*, 1992) and normalized to equal protein concentrations using a BCA assay.

Live-imaging of pH-GluR2L

Rat hippocampal cultures (DIV 12) were transfected with pH-GluR2L or point mutants using lipofectamine (Lin and Huganir, 2007). Imaging was performed as described (Lin and Huganir, 2007). Images were collected at the rate of one image/min from a single optical section (<3 μm) near the surface of the neuron. A Zeiss MultiTime macro was used to correct for focus drift during imaging. Control experiments confirming the specificity of the pHluorin fluorescence signal are detailed in Supplementary data and presented in Supplementary Figure S12.

Statistical analysis

All biochemical experiments were performed at least three times. For neuronal experiments results were obtained from at least two individual platings of neurons. A ChemiDoc XRS system (Bio-Rad) was used for densitometric scanning of X-ray films. Data are expressed as mean ± s.e.m. from the indicated number of experiments. Statistical significance was determined using an unpaired Student *t*-test and significance level is noted in figure legends.

Histograms of pooled data from neuronal biochemical experiments are presented in Supplementary Figure S13.

Supplementary data
Supplementary data are available at *The EMBO Journal* Online (http://www.embojournal.org).

Acknowledgements

We thank Dr T Nieland, other Huganir Lab members and Dr C-Y Su (Yale University) for invaluable comments and K Searcy-Goldberg for excellent technical assistance. This work was supported by a grant from NIMH, R01 MH64856 (R.L.H.)

References

Ashby MC, De La Rue S, Ralph GS, Uney J, Collingridge GL, Henley JM (2004) Removal of AMPA receptors (AMPARs) from synapses is preceded by transient endocytosis of extrasynaptic AMPARs. *J Neurosci* **24:** 5172–5176

Bagowski CP, Besser J, Frey CR, Ferrell Jr JE (2003) The JNK cascade as a biochemical switch in mammalian cells: ultra-sensitive and all-or-none responses. *Curr Biol* **13:** 315–320

Barr RK, Bogoyevitch MA (2001) The c-Jun N-terminal protein kinase family of mitogen-activated protein kinases (JNK MAPKs). *Int J Biochem Cell Biol* **33:** 1047–1063

Bennett BL, Sasaki DT, Murray BW, O'Leary EC, Sakata ST, Xu W, Leisten JC, Motiwala A, Pierce S, Satoh Y, Bhagwat SS, Manning AM, Anderson DW (2001) SP600125, an anthrapyrazolone inhibitor of Jun N-terminal kinase. *Proc Natl Acad Sci USA* **98:** 13681–13686

Besirli CG, Wagner EF, Johnson Jr EM (2005) The limited role of NH2-terminal c-Jun phosphorylation in neuronal apoptosis: identification of the nuclear pore complex as a potential target of the JNK pathway. *J Cell Biol* **170:** 401–411

Bjorkblom B, Ostman N, Hongisto V, Komarovski V, Filen JJ, Nyman TA, Kallunki T, Courtney MJ, Coffey ET (2005) Constitutively active cytoplasmic c-Jun N-terminal kinase 1 is a dominant regulator of dendritic architecture: role of microtubule-associated protein 2 as an effector. *J Neurosci* **25:** 6350–6361

Borsello T, Clarke PG, Hirt L, Vercelli A, Repici M, Schorderet DF, Bogousslavsky J, Bonny C (2003) A peptide inhibitor of c-Jun N-terminal kinase protects against excitotoxicity and cerebral ischemia. *Nat Med* **9:** 1180–1186

Brecht S, Kirchhof R, Chromik A, Willesen M, Nicolaus T, Raivich G, Wessig J, Waetzig V, Goetz M, Claussen M, Pearse D, Kuan CY, Vaudano E, Behrens A, Wagner E, Flavell RA, Davis RJ, Herdegen T (2005) Specific pathophysiological functions of JNK isoforms in the brain. *Eur J Neurosci* **21:** 363–377

Chang L, Jones Y, Ellisman MH, Goldstein LS, Karin M (2003) JNK1 is required for maintenance of neuronal microtubules and controls phosphorylation of microtubule-associated proteins. *Dev Cell* **4:** 521–533

Chen JT, Lu DH, Chia CP, Ruan DY, Sabapathy K, Xiao ZC (2005) Impaired long-term potentiation in c-Jun N-terminal kinase 2-deficient mice. *J Neurochem* **93:** 463–473

Cho KO, Hunt CA, Kennedy MB (1992) The rat brain postsynaptic density fraction contains a homolog of the Drosophila discs-large tumor suppressor protein. *Neuron* **9:** 929–942

Chung HJ, Xia J, Scannevin RH, Zhang X, Huganir RL (2000) Phosphorylation of the AMPA receptor subunit GluR2 differentially regulates its interaction with PDZ domain-containing proteins. *J Neurosci* **20:** 7258–7267

Coffey ET, Smiciene G, Hongisto V, Cao J, brecht S, Herdegen T, Courtney MJ (2002) c-Jun N-terminal protein kinase (JNK) 2/3 is specifically activated by stress, mediating c-Jun activation, in the presence of constitutive JNK1 activity in cerebellar neurons. *J Neurosci* **22:** 4335–4345

Dickens M, Rogers JS, Cavanagh J, Raitano A, Xia Z, Halpern JR, Greenberg ME, Sawyers CL, Davis RJ (1997) A cytoplasmic inhibitor of the JNK signal transduction pathway. *Science* **277:** 693–696

Dong H, O'Brien RJ, Fung ET, Lanahan AA, Worley PF, Huganir RL (1997) GRIP: a synaptic PDZ domain-containing protein that interacts with AMPA receptors. *Nature* **386:** 279–284

Ehlers MD (2000) Reinsertion or degradation of AMPA receptors determined by activity-dependent endocytic sorting. *Neuron* **28:** 511–525

Esteban JA, Shi SH, Wilson C, Nuriya M, Huganir RL, Malinow R (2003) PKA phosphorylation of AMPA receptor subunits controls synaptic trafficking underlying plasticity. *Nat Neurosci* **6:** 136–143

Fogarty MP, Downer EJ, Campbell V (2003) A role for c-Jun N-terminal kinase 1 (JNK1), but not JNK2, in the beta-amyloid-mediated stabilization of protein p53 and induction of the apoptotic cascade in cultured cortical neurons. *Biochem J* **371:** 789–798

Kim MJ, Futai K, Jo J, Hayashi Y, Cho K, Sheng M (2007) Synaptic accumulation of PSD-95 and synaptic function regulated by phosphorylation of serine-295 of PSD-95. *Neuron* **56:** 488–502

Kolleker A, Zhu JJ, Schupp BJ, Qin Y, Mack V, Borchardt T, Kohr G, Malinow R, Seeburg PH, Osten P (2003) Glutamatergic plasticity by synaptic delivery of GluR-B(long)-containing AMPA receptors. *Neuron* **40:** 1199–1212

Kuan CY, Whitmarsh AJ, Yang DD, Liao G, Schloemer AJ, Dong C, Bao J, Banasiak KJ, Haddad GG, Flavell RA, Davis RJ, Rakic P (2003) A critical role of neural-specific JNK3 for ischemic apoptosis. *Proc Natl Acad Sci USA* **100:** 15184–15189

Lee HK, Kameyama K, Huganir RL, Bear MF (1998) NMDA induces long-term synaptic depression and dephosphorylation of the GluR1 subunit of AMPA receptors in hippocampus. *Neuron* **21:** 1151–1162

Lee HK, Takamiya K, Han JS, Man H, Kim CH, Rumbaugh GR, Yu S, Ding L, He C, Petralia RS, Wenthold RJ, Gallagher M, Huganir RL (2003) Phosphorylation of the AMPA receptor GluR1 subunit is required for synaptic plasticity and retention of spatial memory. *Cell* **112:** 631–643

Lee JK, Park J, Lee YD, Lee SH, Han PL (1999) Distinct localization of SAPK isoforms in neurons of adult mouse brain implies multiple signaling modes of SAPK pathway. *Brain Res Mol Brain Res* **70:** 116–124

Lin D-T, Huganir RL (2007) PICK1 and phosphorylation of the AMPA receptor GluR2 subunit regulates GluR2 recycling following NMDA induced receptor internalization. *J Neurosci* **27:** 13903–13908

Malinow R, Malenka RC (2002) AMPA receptor trafficking and synaptic plasticity. *Annu Rev Neurosci* **25:** 103–126

Matsuda S, Mikawa S, Hirai H (1999) Phosphorylation of serine-880 in GluR2 by protein kinase C prevents its C terminus from binding with glutamate receptor-interacting protein. *J Neurochem* **73:** 1765–1768

McCarthy SA, Samuels ML, Pritchard CA, Abraham JA, McMahon M (1995) Rapid induction of heparin-induced epidermal growth factor/diphtheria toxin receptor expression by Raf and Ras oncogenes. *Genes Dev* **9:** 1953–1964

O'Brien RJ, Kamboj S, Ehlers MD, Rosen KR, Fischbach GD, Huganir RL (1998) Activity-dependent modulation of synaptic AMPA receptor accumulation. *Neuron* **21:** 1067–1078

Pearson G, Robinson F, Beers Gibson T, Xu BE, Karandikar M, Berman K, Cobb MH (2001) Mitogen-activated protein (MAP) kinase pathways: regulation and physiological functions. *Endocr Rev* **22:** 153–183

Shepherd JD, Rumbaugh G, Wu J, Chowdhury S, Plath N, Kuhl D, Huganir RL, Worley PF (2006) Arc/Arg3.1 mediates homeostatic scaling of AMPA receptors. *Neuron* **52:** 475–484

Song I, Huganir RL (2002) Regulation of AMPA receptors during synaptic plasticity. *Trends Neurosci* **25:** 578–588

Thiagarajan TC, Lindskog M, Tsien RW (2005) Adaptation to synaptic activity in hippocampal neurons. *Neuron* **47:** 725–737

Thomas GM, Huganir RL (2004) MAPK cascade signalling and synaptic plasticity. *Nat Rev Neurosci* **5:** 173–183

Trinidad JC, Specht CG, Thalhammer A, Schoepfer R, Burlingame AL (2006) Comprehensive identification of phosphorylation sites in postsynaptic density preparations. *Mol Cell Proteomics* **5:** 914–922

Turrigiano GG, Leslie KR, Desai NS, Rutherford LC, Nelson SB (1998) Activity-dependent scaling of quantal amplitude in neocortical neurons. *Nature* **391:** 892–896

Waetzig V, Herdegen T (2005) Context-specific inhibition of JNKs: overcoming the dilemma of protection and damage. *Trends Pharmacol Sci* **26:** 455–461

Whitmarsh AJ, Cavanagh J, Tournier C, Yasuda Y, Davis RJ (1998) A mammalian scaffold complex that selectively mediates MAP kinase activation. *Science* **281:** 1671–1674

Wyszinski M, Kim E, Dunah AW, Passafaro M, Valtschanoff JG, Serra-Pages C, Streuli M, Weinberg RJ, Sheng M (2002) Interaction between GRIP and liprin-alpha/SYD2 is required for AMPA receptor targeting. *Neuron* **34:** 39–52

Xia XG, Hardin T, Weller M, Bieneman A, Uney JB, Schulz JB (2001) Gene transfer of the JNK interacting protein-1 protects dopaminergic neurons in the MPTP model of Parkinson's disease. *Proc Natl Acad Sci USA* **98:** 10433–10438

Yang DD, Kuan CY, Whitmarsh AJ, Rincon M, Zheng TS, Davis RJ, Rakic P, Flavell RA (1997) Absence of excitotoxicity-induced apoptosis in the hippocampus of mice lacking the Jnk3 gene. *Nature* **389:** 865–870

Zhu JJ, Esteban JA, Hayashi Y, Malinow R (2000) Postnatal synaptic potentiation: delivery of GluR4-containing AMPA receptors by spontaneous activity. *Nat Neurosci* **3:** 1098–1106

Zhu JJ, Qin Y, Zhao M, Van Aelst L, Malinow R (2002) Ras and Rap control AMPA receptor trafficking during synaptic plasticity. *Cell* **110:** 443–455

Zhu Y, Pak D, Qin Y, McCormack SG, Kim MJ, Baumgart JP, Velamoor V, Auberson YP, Osten P, Van Aelst L, Sheng M, Zhu JJ (2005) Rap2-JNK removes synaptic AMPA receptors during depotentiation. *Neuron* **46:** 905–916

